Fitting individual-based models of species range dynamics to long-term monitoring data

Anne-Kathleen Malchow[1,*], Guillermo Fandos[1,2], Urs G. Kormann[3], Martin Grüebler[3], Marc Kéry[3], Florian Hartig[4], and Damaris Zurell[1]

[1]Institute for Biochemistry and Biology, University of Potsdam, 14469 Potsdam, Germany
[2]Department of Biodiversity, Ecology & Evolution, Complutense University of Madrid, 28040 Madrid, Spain
[3]Swiss Ornithological Institute, 6204 Sempach, Switzerland
[4]Theoretical Ecology Lab, Faculty of Biology and Pre-Clinical Medicine, University of Regensburg, 93053 Regensburg, Germany
[*]Correspondence author. E-mail: eco@anne-kathleen.malchow.nz

September 26, 2022

Keywords: Bayesian inference; cross-validation; dispersal; inverse calibration; process-based model; range dynamics; spatially-explicit; species distribution model (SDM)

Running title: Fitting IBMs to monitoring data

Target journal: Ecological Applications

Abstract. Generating spatial predictions of species distribution is a central task for research and policy. Among the currently most widely used tools for this purpose are correlative species distribution models (cSDMs). Their basic assumption of a species distribution in equilibrium with its environment, however, is rarely met in real data and prevents dynamic projections. Process-based, dynamic SDMs (dSDMs) promise to overcome these limitations as they explicitly represent transient dynamics and enhance spatio-temporal transferability. Software tools for implementing dSDMs become increasingly available, yet their parameterisation can be complex.

Here, we test the feasibility of calibrating and validating a dSDM using long-term monitoring data of Swiss red kites (*Milvus milvus*). This population has shown strong increases in abundance and a progressive range expansion over the last decades, indicating a non-equilibrium situation. We construct an individual-based model with the RangeShiftR modelling platform and calibrate it using Bayesian inference. This allows the integration of heterogeneous data sources, such as parameter estimates from published literature and observational data from monitoring schemes, and consistent quantification of parameter uncertainties. Our monitoring data encompass counts of breeding pairs at 267 sites across Switzerland over an annual time-series of 22 years. We validate our model using a spatial-block cross-validation scheme and assess predictive performance with a rank-correlation coefficient.

Our model showed very good and excellent predictive accuracy of spatial and temporal projections, respectively, well representing the observed population dynamics over the last two decades. Results suggest that reproductive success was the most decisive factor driving the observed range expansion. According to our predictions, the Swiss red kite population fills most of its range but density will further increase before stabilising mid century.

With our case study we demonstrate the practicality of data integration and validation for dSDMs using available tools. This approach can improve predictive performance compared to cSDMs. The workflow exemplified here can be adopted for any population for which prior knowledge on demographic and dispersal parameters as well as spatio-temporal observations of abundance or occupancy are available. The resulting calibrated model provides refined insights into the ecology of a species and its predictions can inform conservation and management.

1. Introduction

In response to multiple anthropogenic pressures and environmental shifts, the abundance and distribution of many species are changing (Selwood et al., 2015; Newbold et al., 2015; Díaz et al., 2019). Negatively affected populations can potentially be stabilised or even recovered through targeted and effective conservation measures (Hoffmann et al., 2010; Bolam et al., 2021; Duarte et al., 2020). But also expanding populations may be in the focus of conservation interest, for example when exploring scenarios of future threats or evaluating the invasive potential of a species (Thompson et al., 2021). The basis for efficient conservation planning thus lies in reliable knowledge about the spatio-temporal patterns of abundances and the expected effects of conservation measures (Guisan et al., 2013; Zurell et al., 2022).

Various approaches have been developed for spatially-explicit population modelling, ranging from purely correlative to detailed mechanistic species distribution models (SDMs; Dormann et al., 2012; Guisan et al., 2013). Currently, most spatial model assessments for conservation planning are based on projections of correlative SDMs (cSDMs) (Franklin, 2013; Zurell et al., 2022), that statistically relate species occurrences to environmental predictors (Elith & Leathwick, 2009). This class of models can achieve high flexibility and may be readily fitted to available occurrence data, but their geographical and temporal transferability is limited (Araújo & Peterson, 2012; Wenger & Olden, 2012). They further provide only stationary or time-implicit predictions, which rely on the assumption that the observed distribution is in equilibrium with its environment (Guisan & Thuiller, 2005). However, this assumption is commonly violated in conservation-relevant cases such as invasive species, reintroduction programs, or threatened populations that are subjected to ongoing environmental change. This leads to inaccurate projections because the true species distribution is actually transient and thus dependent on time and history (Santos et al., 2020; Watts et al., 2020; Semper-Pascual et al., 2021).

Present species distributions and abundances are generally the result of the effects and interplay of a number of eco-evolutionary processes (Urban et al., 2016). To reflect this, dynamic spatially-explicit process-based SDMs (hereafter called dSDMs) include an explicit description of at least one of these processes to model the spatio-temporal and potentially transient dynamics of population abundance. Examples include representations of local population dynamics (Keith et al., 2008; Barber-O'Malley et al., 2022) and limiting processes like dispersal (Risk et al., 2011; Broms et al., 2016; Smolik et al., 2010), physiology (Rodríguez et al., 2019), or species interactions (Schweiger et al., 2012; Pellissier et al., 2013). Further,

dSDMs often include stochastic elements to account for processes not explicitly described by the model. Thanks to the integration of ecological theory, dSDMs are expected to provide more accurate predictions under extrapolation and thus to be more readily transferable to non-analog conditions than cSDMs (Gallien et al., 2010).

To date, the widespread use of dSDMs for conservation applications has been hampered by technical challenges related to their parameterisation and validation (Briscoe et al., 2019). Fully specifying a dSDM includes two main steps, both of which require various types of knowledge about the population of interest (Singer et al., 2018; Fig. 1). First, in the model building step, the model structure and the functional description of the included processes are established. They are usually chosen based on ecological theory and expert opinion. Second, in the parameterisation step, the numeric values of all process rates, such as demographic and dispersal rates, are determined by direct or inverse (indirect) parameterisation or a combination of both. Direct parameterisation uses estimates of process parameters based on data collected in the field or from experiments. Conversely, inverse parameterisation is based on spatio-temporal observations of the modelled response variables, typically abundance or occurrence. To make efficient use of all sources of information and combine direct and inverse parameterisation, a Bayesian calibration framework can be employed. Here, the direct parameterisation and its uncertainty are expressed as prior distributions. These priors are updated by a likelihood, that measures how well a given set of parameter values is able to reproduce the observed response data. This yields the posterior distribution via Bayes' rule. Thus identifying parameterisations that are supported by the data can generate new knowledge on the studied population, as prior estimates of process parameters are corrected and their uncertainty may be reduced. This approach allows the consistent propagation of uncertainty from the data sources through to model predictions (Hartig et al., 2012; Marion et al., 2012; Jaatinen et al., 2021; Heard et al., 2013). It is therefore ideally suited for linking process-based models with monitoring data to obtain a solid quantitative basis for management decisions while being explicit, and honest, about all uncertainties involved (Zylstra & Zipkin, 2021).

Effective and accessible tools for building and calibrating different types of dSDMs are becoming increasingly available and render the application of complex modelling workflows feasible (Hartig et al., 2019; Visintin et al., 2020; Malchow et al., 2021; Fordham et al., 2021). Here, we tested their applicability by fitting the individual-based modelling (IBM) platform RangeShiftR (Malchow et al., 2021) to long-term survey data with a Bayesian calibration approach (Hartig et al., 2019). As a case study we modelled the Swiss population of the red kite (*Milvus milvus*), an iconic bird of prey that is almost endemic to Europe. This species has

a highly dynamic population history, as its fate has been strongly marked by anthropogenic influences during the past centuries. In the 19th century it has suffered heavy declines throughout its range due to human persecution, leading to concerningly low abundances and regional extinctions during the first half of the 20th century and until the 1970s, when the species was classified as globally endangered (Evans & Pienkowski, 1991). Thanks to legal protection, effective conservation measures and reintroduction projects, e.g. in the UK and Italy, the total range and population abundances of the red kite have widely recovered. Switzerland now harbours about 10% of the global population (Aebischer & Scherler, 2021) and has seen accelerating population increases in recent years (BirdLife International, 2021). However, trends are inconsistent across the European populations with declines in Spain, stable populations in France, Germany and Poland, and increases in Great Britain, Sweden and Switzerland (Mattsson et al., 2022). Both ongoing threats, like illegal killing and poisoning, as well as novel threats, for example wind turbines and electrocution at power lines, have the potential to substantially increase adult mortality (Bellebaum et al., 2013; Schaub, 2012; Mattsson et al., 2022). Thus, in line with proactive conservation planning that anticipates and ideally averts negative trends, it is important to identify key determinants of red kite distribution at management-relevant scales in order to design early and effective conservation measures. dSDMs can play a central role in this task, as they link observed abundances with underlying processes in a mechanistic manner (Fordham et al., 2013).

In this case study, we calibrated and validated a dSDM of the red kite in Switzerland that consisted of a mechanistic IBM and explicitly simulated population dynamics and dispersal. In the following, we describe how we used published literature data and expert opinion to directly parameterise the model. This parameterisation was subsequently updated by integrating information from long-term, structured survey data in a Bayesian inference. Based on this, we investigated which process parameters were most influenced from the survey data. Comparing the prior and posterior predictions of our model, we found that the calibration considerably improved the fit and reduced uncertainty. The fitted model was validated using spatial block cross-validation (Roberts et al., 2017), where its predictive performance exceeded that of a comparable cSDM (Briscoe et al., 2021). The model was further used to make predictions of future abundance and distribution. The workflow shown here (Fig. 1) can guide the application of complex dSDMs to any population that exhibits variable dynamics and for which suitable data sources for direct and inverse parameterisation are available.

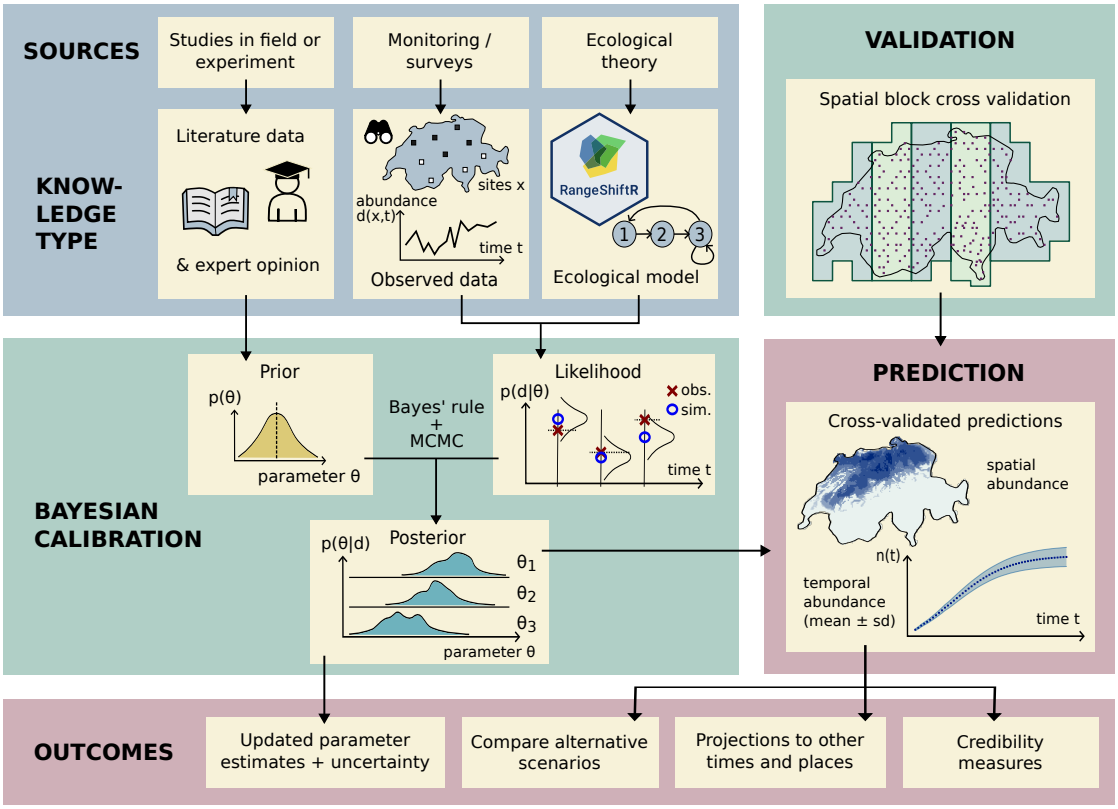

Figure 1: Calibration and validation workflow for process-based, dynamic species distribution models. Different types of knowledge are needed to construct and parameterise the model. Direct knowledge of the model parameters can be combined with observations of the model's response quantity via a likelihood function within a Bayesian inference framework. To generate cross-validated predictions, the calibration is repeated for each spatial block, using the data of the latter as a hold-out data set that is then predicted and compared to observations through a performance measure. Various outcomes can be derived, both from the posterior distribution directly and from model predictions.

2. Materials and Methods

2.1. Data

We utilised two sources of monitoring data of the red kite across Switzerland: the Swiss breeding bird atlas that provides snapshot data from two periods (1993-1996, Schmid et al. (1998); and 2013-2016, Knaus et al. (2018)) and the Swiss breeding bird survey (MHB, Schmid et al., 2004) that provides abundance time series for the years 1999-2018. Both schemes are based on so-called simplified territory mapping of representative 1 km^2 squares

across Switzerland and record the number of observed breeding pairs during two to three repeat surveys per year along a fixed survey route in each square (Schmid et al., 2004). The Atlas survey data used here included 2318 sites, each of which is sampled in one year within each five-year period. The MHB survey includes 267 sites (1 km^2 sampling quadrats) laid out across Switzerland in a regular grid, which are sampled yearly since 1999. Further, we used land cover and bioclimatic data as environmental predictors. The land-cover data was obtained from the CORINE project (European Union, 2022) for the years 2000, 2006, 2012, and 2018 at a resolution of 100 m. The bioclimatic data is obtained from CHELSA Bioclim v1.2 (Karger et al., 2017; Karger et al., 2016) and covers the time period 1979–2013 with a resolution of 30 arcsec ($\approx$ 1 km).

2.2. Modelling

Our dSDM comprised two components: a static habitat model that describes the habitat suitability in each year over the study region and a mechanistic individual-based model (IBM; Railsback & Grimm, 2019) that describes the population and range dynamics. IBMs use a bottom-up approach in which key processes are described at the individual level (DeAngelis & Mooij, 2005) that can be scaled up to the population level by numerical simulation. All analyses were conducted using the statistical programming language R (R Core Team, 2020).

2.2.1. Habitat suitability of the Swiss landscape

Habitat suitability was derived from a cSDM based on presence-absence data generated from the second atlas (2013-'16) data set. Because the red kite has been expanding its range in Switzerland during the past 30 years, this most recent data best reflects the underlying habitat requirements. For the cSDM, we assumed that most suitable habitats are already occupied even though they may not have reached their potential capacities yet. The red kite is a generalist and opportunistic raptor breeding in a wide range of climates and habitats. Typical nesting habitat consists of forest patches with suitable roosting sites and open areas like grassland or agricultural fields that provide prey, which mostly consists of small mammals. Food sources like open waste dumps and carrion are readily exploited if present. To represent the availability of resources relevant for the occurrence of red kites, we used the CORINE 2012 land cover data with its 44 classes aggregated to seven land cover types (Table A.1). To represent climatic influences, all nineteen Bioclim variables were included (Table A.2). Since the red kite requires different habitats for nesting and foraging, it is a highly mobile species and occupies breeding home range sizes of about 4 to 5 km^2 for males (Baucks, 2018;

Nachtigall, 2008). To allow the cSDM to consider the diversity of habitat types, we used a grid cell size of 4 km^2. As the entire dSDM is based on this grid, this also constitutes a trade-off between the abilities to resolve both the effects of density-dependence on the one hand and dispersal displacements on the other hand. The high-resolution land cover data was aggregated to the target resolution of 2 km by calculating the proportional land cover in each cell. The bioclimatic data was coarsened to the 2 km-resolution by bi-linear interpolation between the grid cells.

To fit the cSDM, we first selected predictors from all land-cover and bioclimatic variables based on their univariate importance (assessed by the AIC of linear models with second-order polynomials) under the constraint that pairwise Spearman correlation must not exceed 0.7 (Dormann et al., 2013). The variables selected are labelled with an asterisk in Tables A.1 and A.2. We then created an ensemble cSDM by taking the mean occurrence probability predicted by four different algorithms: binomial linear model with second-order polynomials and step-wise variable selection; binomial additive model with splines; random forest; and boosted regression trees. The predicted probabilities are subsequently interpreted as a habitat suitability index (HSI). The ensemble cSDM was then projected to Switzerland and a 12 km buffer around its border for the years 2000, 2006, 2012, and 2018, for varying land-cover data and constant bioclimatic variables. Climate was kept constant as its change was considered only a minor driver of the observed range dynamics. The buffer was used to reduce potential boundary effects in the IBM simulations. It was large enough to capture most dispersal events in the Swiss population. For all other years in the period of 1999-2020, the HSI values were linearly interpolated. To distinguish between habitat and non-habitat cells, we derived a binarisation threshold ($\widehat{\text{HSI}}$ =0.51) as the value yielding equal sensitivity and specificity ($\approx$ 90%) and considered all cells with lower HSI values non-habitat.

2.2.2. Individual-based model

We used the R-package RangeShiftR (Malchow et al., 2021), that interfaces to the individual-based modelling platform RangeShifter 2.0 (Bocedi et al., 2021), to construct a dSDM based on the gridded habitat suitability maps described above. In the following, we describe the main steps of the direct parameterisation, and refer to the full ODD (Overview, Design concepts and Details) protocol (Grimm et al., 2020) in the Appendix (SI B) for all details. RangeShiftR explicitly simulates demography and dispersal in discrete unit-time steps, which here describe one year. During each year, the processes "reproduction", "juvenile dispersal", "survival", "development", and "aging" are evaluated in this order for all individuals. The prior distributions on the respective process parameters (Table 1) were informed by literature

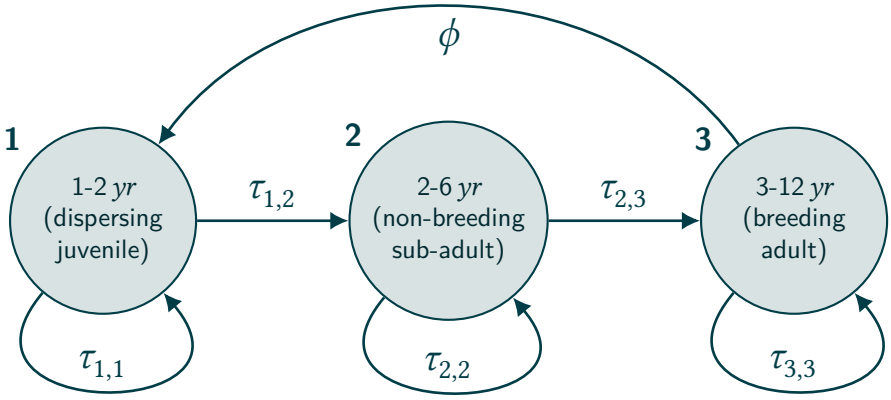

Figure 2: Life-cycle graph of the stage-structured population model for the red kite with three developmental stages. The probability for an individual in stage s to stay in its stage over one time step (1 year) is denoted by $\tau_{s,s}$, and to move to the next stage is denoted $\tau_{s,s+1}$. Only stage 3 produces offspring, with a fecundity of ϕ.

Table 1: Process parameters included in the Bayesian calibration and the parameters of their truncated normal prior distributions.

Parameter name	**Lower bound**	**Mean**	**SD**	**Upper bound**
Density-dependence b^{-1}	0.001	0.006	0.0025	0.020
Fecundity ϕ_0	0.5	1.66	0.51	5.0
Survival prob. σ_1	0.01	0.42	0.08	0.99
Survival prob. σ_2	0.01	0.68	0.09	0.99
Survival prob. σ_3	0.01	0.80	0.05	0.99
Development prob. $\gamma_{1\to2}$	0.01	0.80	0.10	0.99
Development prob. $\gamma_{2\to3}$	0.01	0.55	0.10	0.99
Emigration prob. e_1	0.01	0.80	0.10	0.99
Settlement inflection pt. β_s	−15.0	4.0	4.0	15.0
Dispersion parameter ν	1.0	50.0	250.0	500.0

data and expert knowledge. They were then updated with information contained in the survey data via Bayesian inference as described below.

Our model is female-based, since females primarily determine the population dynamics. Their development is described in three stages (Fig. 2), with classifications and age ranges adopted from Sergio et al. (2021) and Newton et al. (1989): Dispersing juveniles are one to two years old, sub-adults establish a territory within their second to sixth year, and breeding adults can be as young as three but maximally twelve years of age. A senescent stage was not included in the model because it does not contribute to the overall fecundity and non-breeding adults are not monitored in the survey. The age limits are not strict, as the stage transitions are modelled probabilistically (Fig. 2). The transition probabilities $\tau_{m,n}$ are expressed as survival probabilities of stage s, $\sigma_s = \tau_{s,s} + \tau_{s,s+1}$, and the development probabilities $\gamma_s = \tau_{s,s+1}\,\sigma_s^{-1}$, that can independently vary between zero and one. The latter are assumed as $\gamma_1 = 0.80 \pm 0.10$ for stage 1 and $\gamma_2 = 0.55 \pm 0.10$ for stage 2, to approximately yield the given age classes (Fig. A.1). The survival probabilities σ are taken from Katzenberger et al. (2019) for all three stages: $\sigma_1 = 0.42 \pm 0.08$ and $\sigma_2 = 0.68 \pm 0.09$ and $\sigma_3 = 0.80 \pm 0.05$, which is also in accordance with Schaub (2012) and Newton et al. (1989).

Fecundity ϕ was assumed to be density-dependent and was modelled as an exponential decay with population density. Each cell i is characterised by a local strength of demographic density-dependence b_i, which is obtained as the global strength b divided by the cell habitat suitability HSI_i, $b_i = b\ \mathrm{HSI}_i^{-1}$, given in units of cell area ($a_c = 4$ km^2). Fecundity follows the relation $\phi_i(n_i) = \phi_0\,\mathrm{e}^{-b_i n_i}$, where n_i denotes the density of adults in stages 2 and 3 in cell i (i.e. juveniles do not count towards this density-dependence). The base value ϕ_0 is the required process parameter and denotes the theoretical fecundity at zero population density. Nägeli et al. (2021) report a realised fecundity of 1.77 ± 0.70, which agrees with Schaub (2012) and Nachtigall (2008). We assumed that this value is reached at a density of 25 breeding pairs (BP) per 100 km^2 (i.e. 1 BP per cell) and halved it for our female-only model: $\phi_1 = \phi(n = 1/a_c) = 0.88 \pm 0.35$. We can then get ϕ_0 as $\phi_0(b) = \phi_1\,\mathrm{e}^{b/\mathrm{HSI}}$, with b as a calibration parameter that controls the degree of density-dependent decay in fecundity. The HSI over all habitat cells had a mean and standard deviation of $80\% \pm 12\%$ and we assumed that the lower and higher fecundities were attained in the lower and higher quality habitats. This was given with a range of $b = (0.50 \pm 0.15)\,a_c$ (Fig. A.2), yielding $\phi_0 = 1.65 \pm 0.51$.

Dispersal is explicitly modelled in three stages: emigration, transfer and settlement (Travis et al., 2012). Red kites are strongly philopatric (Newton et al., 1989) so that emigration was modelled as occurring in the first stage only. The emigration probability was assumed constant at $e_1 = 0.64 \pm 0.10$, meaning that an expected proportion of 87% of juveniles have

dispersed in year three. This value best matched observations in which 42% of females of a cohort have emigrated after year one and 45% after year two (own unpublished data), suggesting a larger proportion of emigrants among two-year-old juveniles than one-year-old juveniles. The transfer phase described the movement of a dispersing individual through the landscape. It was modelled as a strongly correlated random walk in a random direction with a step length equal to the cell size. After each step, the option to end the movement and settle was evaluated. Settlement was only possible in habitat cells and its probability was density-dependent with a sigmoid relationship (Fig. A.3). Its inflection point β_s was a calibrated parameter and was estimated as $\hat{\beta}_s = \beta_s/b = (4 \pm 4)\, a_c^{-1}$. The maximum settlement probability and the slope parameter were both fixed parameters and were assumed as $\alpha_s = -1$ and $s_0 = 0.75$, respectively. The maximum number of steps in the random walk was set to 10. Therefore, depending on the availability of sparsely populated habitat, individuals exhibit dispersal distances between 2 and maximal 20 kilometres, which is consistent with observations (own unpublished data; Newton et al., 1989; Nachtigall, 2008). Longer-range dispersal events are also frequently observed, but excluded from the model due to the small study region and the mountainous terrain. In- or outflux of individuals across the system boundaries was not considered.

The initial conditions of each simulation were stochastic. The number of adult individuals in each cell was drawn from a Poisson distribution whose mean values were predicted from a generalised linear model. This model of the initial red kite distribution was an autoregressive distribution model (Dormann et al., 2007) of the earlier atlas data (1993-'96) with the spatially interpolated values of atlas counts as its sole predictor (Fig. A.4). The number of juveniles and sub-adults was subsequently estimated from the demographic rates under the assumption of a stable stage distribution.

2.3. Bayesian calibration

In a Bayesian calibration, a joint posterior distribution was estimated for nine model parameters θ based on their prior distributions $p(\theta)$ and the likelihood $l(\theta)$ (Fig. 1). The priors express the a-priori information that we assumed about likely parameter values as summarised in Table 1. The likelihood function $l(\theta)$ measures the fit of the model M, parameterised with θ, to the monitoring data. The calibrated model parameters are: the strength of density-dependence $1/b$; six demographic probabilities for survival of all stages (σ_1, σ_2, σ_3), juvenile and sub-adult development ($\gamma_{1\to2}$, $\gamma_{2\to3}$), and the base adult fecundity (ϕ_0); as well as two dispersal parameters to control the emigration (e_1) and settlement probabilities (β_s). Additionally, a dispersion parameter ν is calibrated, which is introduced below.

All priors $p(\theta)$ were chosen as truncated normal distributions. Their means and standard deviations were informed from the literature and expert opinion and they were bounded to their respective valid parameter ranges (Table 1). As calibration data, we used the observed abundances from the MHB survey, D_{MHB}. Based on this data, we defined a likelihood $l(\theta) = p(D_{\text{MHB}} \,|\, \theta, M)$ as follows: For a given parameter vector θ, the RangeShiftR simulation model (M) is run and the output abundance data are aggregated and averaged over twenty replicate runs of the model. The result D_{sim} is compared with the MHB data under the assumption of a negative-binomial error distribution, so that for an observation at site i and time t, $l_{i,t}(\theta) = Pr_{\text{NB}}(D_{\text{MHB,i,t}} \,|\, \mu{=}D_{\text{sim,i,t}}, \nu)$. The parameter ν describes the error over-dispersion and was also calibrated. It arises in an alternative formulation of the negative-binomial probability mass function Pr_{NB} formulated in terms of its mean μ and dispersion ν, instead of the success probability $r = \nu/\mu{+}\nu$ and the target number of successes $n = \nu$. Therefore, its variance is given by $\sigma^2 = \mu + \mu^2/\nu$. It approaches μ from above when $\nu \to \infty$ and the negative binomial converges to the Poisson distribution. The variance can thus be tuned with ν, rendering it an appropriate description of observation error for over-dispersed count data.

Due to the stochasticity inherent in our simulation model, the likelihood values were also stochastic. For the applied Markov chain Monte Carlo approach (MCMC, details below), this is conceptually not a problem since the pseudo-marginal theorem guarantees that the MCMC sample still converges to the correct posterior distribution (Warne et al., 2020). Practically, however, large variances in the likelihood will increase the convergence time dramatically, as the sampler gets stuck for occasional high likelihood values. To reduce the stochasticity in the likelihood, we aggregated the abundance data within spatio-temporal blocks of 14×14 grid cells in space and three years in time (Figs. A.5 and A.6). These aggregation factors were chosen with the target of reaching a variance below ten in repeated likelihood evaluations for a given Θ. The aggragation resulted in 57 spatial and 5 temporal blocks, within which the observed and simulated red kite densities were compared. Under the usual independence assumptions, the total likelihood was then expressed as the product over all blocks: $l(\theta) = \prod_{i=1}^{57} \prod_{t=1}^{5} l_{i,t}(\theta)$.

To validate the calibration setup and assess the sensitivity of the likelihood $l(\theta)$ to changes in the model parameters θ, we performed a local sensitivity analysis (Fig. A.7). For this, a test data set D_{SA} was simulated from the model with all parameters at their mean prior values. Then, one parameter at a time was varied within the boundaries of its prior distribution while keeping all other parameters at their mean and evaluating the likelihood with respect to D_{SA}. Further, we performed a global sensitivity analysis with Morris' elementary effects screening

method (Morris (1991); Fig. A.8). Based on these analyses, we expected that the strength of density-dependence $1/b$, the adult base fecundity ϕ_0 and the three survival probabilities σ will calibrate best under our setup, whereas the development probabilities γ and the emigration probability would be only weakly informed by our survey data through the specified likelihood.

To estimate the joint posterior distribution based on the defined $p(\theta)$ and $l(\theta)$, we used a MCMC sampling scheme (Luengo et al., 2020). Therein, the posterior density $p(\theta | D_{\text{MHB}}, M)$ of a given parameter set θ is evaluated according to Bayes' rule. The chosen MCMC algorithm was a type of adaptive Metropolis sampler, the differential evolution sampler with snooker update (DEzs, Braak & Vrugt, 2008), as implemented in the BayesianTools R-package (Hartig et al., 2019). Every calibration run included three independent DEzs-MCMCs with a length of 2×10^5 iterations, of which the first 5×10^4 were discarded as an initial burn-in period. Each DEzs, in turn, consisted of three inter-dependent internal chains, meaning each calibration comprised a total of nine chains.

2.4. Spatial block cross-validation

We employed a spatial block cross-validation scheme to evaluate the model fit without duplicate use of data for both model calibration and validation (Roberts et al., 2017). To this end, the data was split into five spatially contiguous folds (Fig. 1 and Fig. A.5), for each of which the respective subset of MHB data was held out and the model was fit to the remainder of the data. We chose longitudinally structured folds to capture a similar altitudinal profile and thus a largely identical set of environmental conditions within each one. For subsequent model validation, the respective calibration results for each fold were used.

Posterior model projections were generated by taking a sample of 1000 draws from the joint posterior, running the dSDM with each drawn parameter vector, and calculating the mean, median and 95%-credibility interval (CI) of the simulated abundances. Prior predictions were obtained in the same way but using draws from the prior distribution. Both prior and posterior predictions were run for the time covered by the MHB data and 30 years further into the future, i.e. from 1999 to 2050.

To assess the model fit, we calculated Harrell's c-index (Newson, 2006, using the function *rcorr.cens* from the Hmisc R-package), a rank correlation index that generalises the AUC index to non-binary response variables. It quantifies the probability that for a given pair of data points the ranking of predictions matches the ranking of observations. This measure was used in Briscoe et al. (2021) as a form of temporal AUC to assess the prediction performance of temporal trends. We use it here as an index that is applicable to abundance predictions

and can be interpreted like the AUC for occurrence predictions.

3. Results

3.1. Posterior distributions

The DEzs-MCMCs were checked for convergence using trace plots (A.9), trace rank plots (Vehtari et al. (2021), Fig. A.10) and the potential scale reduction factor (psrf; Gelman & Rubin (1992), Fig. A.11). They were considered approximately converged if their multivariate psrf value had dropped below 1.10. However, there were considerable differences between the folds due to a varying number of MHB sites included, and the chains reached psrf values of 1.05, 1.02, 1.05, 1.09, and 1.04, respectively, for folds 1 to 5.

The marginal posterior distributions for each parameter and each spatial fold are represented by box plots in Fig. 3. The marginal distributions for a calibration with the complete data set are shown in Fig. A.12. A comparison between the respective prior and posterior reveals how the consideration of the survey data changes the initial parameter estimates that were obtained directly from literature data. Notably, the medians of the marginal distributions for fecundity and the survival probabilities of the first and second stage have shifted significantly, whereas those of the other parameters remained largely unchanged. However, not only the point estimates but also their uncertainty can change by including more information. To evaluate if and by how much the uncertainty was reduced, we assessed the breadth of the marginal distributions of each calibrated parameter by calculating the width of the highest-posterior-density intervals (HPDIs) and compared them for the prior and posterior distributions Fig. A.13. We found substantially narrower posteriors for the strength of density dependence $1/b$, fecundity ϕ_0 and the survival probabilities of stages one and two, σ_1 and σ_2, which all already responded strongly in the sensitivity analysis. No uncertainty reduction nor any significant change in the point estimate was found for adult survival σ_3, contrary to our expectation based on the sensitivity analysis, but this parameter had already had the most informative priors to begin with. The dispersion parameter of the negative binomial error model was calibrated to a very large value, yielding a variance that was close to that of a Poisson distribution. Thus, only slight over-dispersion was detected relative to a Poisson. The variance of posteriors over the five folds was very small and there were no significant differences in point estimates.

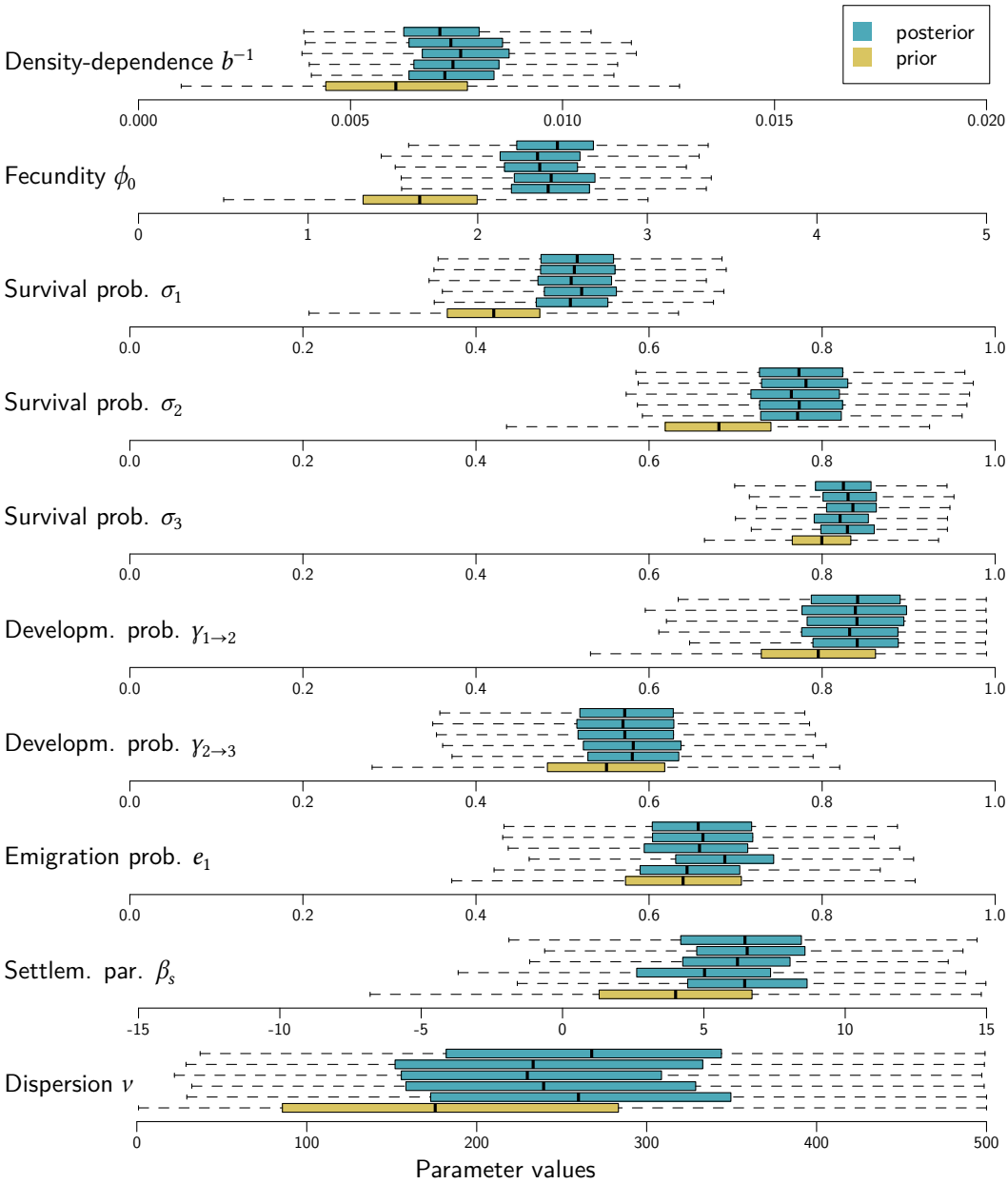

Figure 3: Box plots summarise the marginal prior (yellow) and posterior (blue) distribution for each calibration parameter and for all five spatial folds. The black bar marks the median, the boxes show the inter-quartile range, the whiskers extend to the most extreme data point which is no further away from the box than 1.5 times its length.

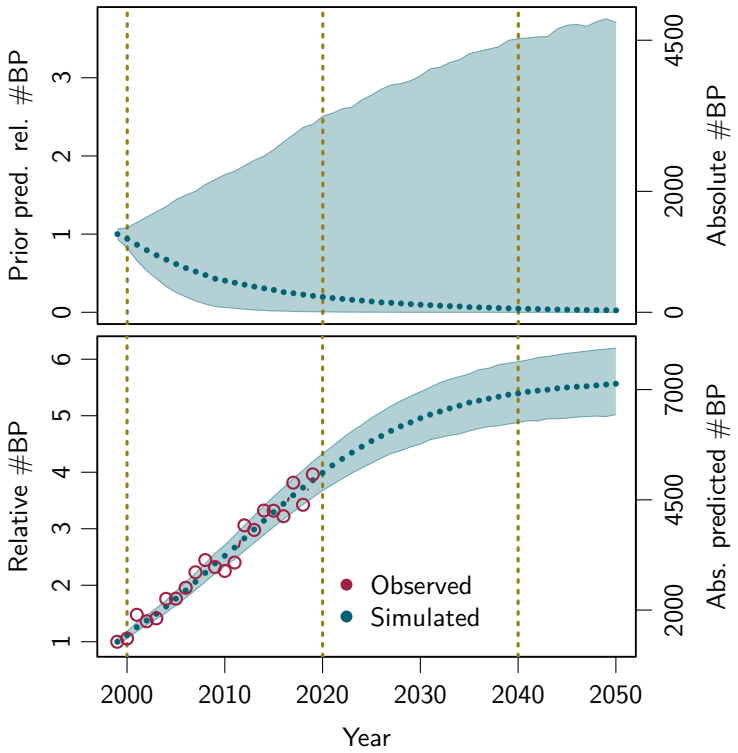

Figure 4: Prior (top) and posterior (bottom) predictions of the abundance time series of red kite in Switzerland. The blue line and band show the median and 95%-credibility interval of total number of predicted breeding pairs (#BP), with relative values (with respect to year 1999) on the left and absolute values on the right y-axis. The bottom panel shows the cross-validated posterior predictions together with the breeding bird index (red circles, relative y-axis only) for comparison. The dashed vertical lines mark the years for which spatial predictions are depicted in Fig. 5.

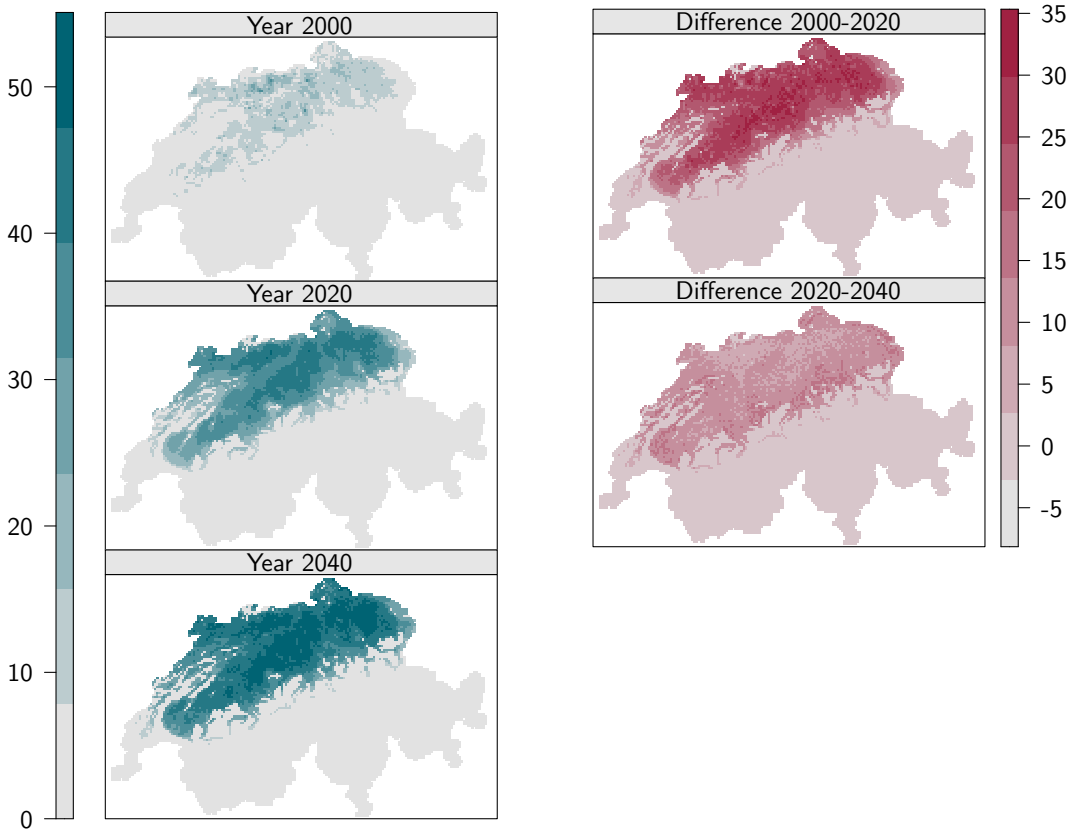

Figure 5: Cross-validated mean predicted population densities for the years 2000, 2020, and 2040 (left column) and the differences between those years (right column). The unit of the colour scales is number of breeding pairs per 100 km^2.

3.2. Validation & Predictions

To assess the benefit gained from the inverse calibration step compared to only direct parameterisation, Fig. 4 shows the prior and posterior predictions of red kite abundance time series from 1999 to 2050. Simulations from the prior show negative population trends in most cases, but they also have a large 95%-CI that includes predictions of zero to 3500 breeding pairs in the year 2020. The posterior predictions, in contrast, show increasing trends and a much narrower CI. For comparison, we also depicted the breeding bird index, that quantifies the population trend relative to the year 1999 (Knaus et al., 2022).

For model validation, the c-index was computed for different subsets of the data. First, it was calculated over all observations, i.e. all combinations of site and year, within each

fold. The results were quite variable and ranged from 0.71 to 0.94 (Fig. A.15), which is likely due to the differing number and information content of the included MHB sites. The sample-size weighted mean c-index was 0.86, which indicates an excellent fit to the validation data. Second, focusing on regional abundance dynamics, we also calculated the c-index for the time series of the total abundance within each fold, yielding consistently high values of 0.92 to 0.94 (mean 0.93; Fig. A.16). This confirms that averaging the abundance over large regions further increases the accuracy of temporal predictions. Third, we were interested in the performance of our dSDMs at those MHB sites that showed the highest variance in their red kite counts, since highly variable time series are harder to predict. To this end, we ranked all MHB sites by their count variance and looked at the c-index of the top 15% most variable sites. We found values between 0.71 and 0.78 (mean 0.75; Fig. A.17), which signifies a substantial drop in performance but still indicates acceptable predictions at highly variable sites.

The model projections were also used to generate predictions to places and times not covered by the MHB survey. Fig. 4 shows the cross-validated prediction of total red kite abundance during the entire survey period and 30 years into the future. These results suggest that the steepest increase in abundance occurred over the recent twenty years and that the next two decades will see slower population increases which stabilise towards 2050. Spatial predictions were made to the whole country (Fig. 5) as three snapshots in time: at the beginning (2000) and end (2020) of the survey data set, as well as a further twenty years into the future (2040). Over the past two decades, the model predictions mirror the strong range expansion of the red kite range in Switzerland, whereas the coming two decades will be characterised by an increase in density in the newly colonised areas. The same maps were created from prior predictions for further comparison (Fig. A.18) and they exhibit a contracting range over time indicating substantial deviation between direct and inverse calibration. Since the fecundity and early survival rates responded most strongly to the calibration, it is suggested that the reproductive success plays a major role in driving the resulting increases in local density and distribution.

4. Discussion

Reliable methodology for understanding and predicting a species' population and range dynamics will be crucial to inform decision making in the future. Dynamic, spatially-explicit, process-based distribution models (dSDMs) provide valuable advances towards improved biodiversity forecasts (Urban et al., 2016) but are currently underused due to technical and

data challenges and limited guidance for applications (Briscoe et al., 2019; Zurell et al., 2022). This study contributes to overcoming these challenges. We demonstrated the practicability of a complete modelling workflow for dSDMs with a case study of a conservation-relevant population, the red kite in Switzerland. This included calibrating the RangeShiftR IBM, a complex simulation model, to heterogeneous empirical data, interpreting the results, and validating the model by cross-validation in a spatial block design. Thanks to the use of Bayesian inference, we can integrate direct and indirect knowledge on the process parameters, account for their uncertainty and propagate it to model predictions. Our model captures the Swiss red kite population trends with higher spatial and temporal predictive accuracy than achieved with correlative models in a previous study (details below, Briscoe et al., 2021). The model predicts a continued population growth which stabilises towards the middle of the century. The workflow exemplified here can be readily adapted to other species, if population prior parameter estimates as well as response data (e.g. occupancy or abundance data) are available, and promises to yield improved parameter estimates and more accurate, validated model predictions.

For this case study of the red kite in Switzerland, we built a process-based dSDM using the individual-based modeling platform RangeShiftR (Malchow et al., 2021). It explicitly considers relevant ecological processes such as demography and dispersal and includes further influential effects such as density-dependence. Therefore, transient dynamics, that arise when a distribution is not in equilibrium with its environment, can be accommodated and complex dynamics can be represented. The IBM structure was determined based on expert opinion and the direct (prior) parametrisations of the process parameters were derived from literature data. IBM approaches are particularly suited for the direct estimation of their parameters (e.g. survival probability or dispersal distance) because they formulate all processes from the perspective of the individual (Railsback & Grimm, 2019), where they can be estimated from data obtained in observational studies (e.g. mark-recapture). The prior estimates were updated using the MHB survey data within a Bayesian inference. Here, IBMs have the advantage of realistically modelling small local populations of a few individuals by incorporating demographic stochasticity, so that the survey data can be used at a high spatial resolution.

Because in dSDMs the calibrated parameters have a well-defined ecological meaning, their estimation itself can produce new insights. With our case study of the red kite in Switzerland, we found that some parameters in particular, e.g. the adult fecundity ϕ_0, its density-dependence $1/b$, and the survival probabilities of juveniles and sub-adults, σ_1 and σ_2, responded strongly to the inclusion of additional information from survey data. This behaviour was predicted well from the local and global sensitivity analyses. The detected sensitivity

further indicates that the model projections are responsive to these parameters, thereby suggesting potential pathways for conservation measures, e.g. highlighting the protection of young individuals and supporting nest success. The prior estimate of $1/b$ was corroborated and those of ϕ_0, σ_1 and σ_2 were corrected to higher values, while the uncertainty around all four estimates was reduced. The discrepancies found between prior and posterior estimates can be explained by different factors (Cailleret et al., 2020): Firstly, there can be a true difference, for example, if estimates are obtained from different study populations. In our case, the prior fecundity was based on a measurement from a Swiss sub-population with a high breeding density, which may have a lower fecundity than the Swiss average. The prior survival probabilities are taken from a German red kite population, that shows a slightly negative population trend, and the upward correction seems to better match the increasing Swiss population. Red kite in Switzerland benefit from public feeding (Cereghetti et al., 2019) and many sub-adult individuals change from migratory to resident behaviour, which can also increase survival. Secondly, an important source of deviations between empirical and calibrated parameter estimates is model error. Our IBM captured only a subset of the multiple eco-evolutionary processes that underlie the observed abundance patterns. Therefore, the calibrated parameters will account for missing processes to some extent. This highlights the need for further development of dSDMs to include more mechanisms and thus to fit observed data more closely. It further emphasises the importance of effective integration of direct and inverse calibration to estimate parameter values and their uncertainties, since predictions and derived management decisions can be highly sensitive to the final parameterisation.

The validation of model predictions (Araújo et al., 2005) is common practice in the application of cSDM but is often missing with dSDMs. Here, we have successfully adapted spatial-block cross-validation to an IBM by calibrating the model to each of five spatially contiguous regions within the study area. However, performing a cross-validation is usually computationally expensive, as the calibration needs to be repeated for each set of hold-out data. Further, if the folds are not selected carefully, it bears the risk of limiting the environmental conditions represented in each calibration, which can cause extrapolation issues in the model evaluation. Therefore, a suited validation method has to be chosen carefully. Alternatives include cross-validation with random instead of blocked folds (Roberts et al., 2017) and approximations to leave-one-out validation by WAIC (Vehtari et al., 2017).

The total red kite model was evaluated based on its cross-validated abundance predictions using Harrell's c-index as a measure of predictive performance, which indicated excellent predictive accuracy. In sites with highly fluctuating abundances performance dropped considerably, but still provided acceptable predictions. A similar analysis was conducted by Briscoe

et al. (2021) who compared the accuracy of correlative SDMs and dynamic occupancy models (Kéry et al., 2013) that were fitted to the MHB data of 69 Swiss birds, including the red kite. They found that predictive ability of occupancy was high for all examined model types when assessed across all sites (mean AUC > 0.8) but much lower when specifically testing only sites that showed occupancy change (mean AUC 0.64-0.71). The AUC metric is based on predictions of occupancy only and therefore generally scores above the c-index, which ranks abundances. Collapsing our abundance predictions to occupancy and comparing them to Briscoe et al. (2021) in terms of the AUC, our calibrated IBM surpasses the mean of their red kite SDMs, both across all sites (0.91 versus 0.85) and occupancy-switching sites only (0.80 versus 0.67). Especially in range shifting populations, such as the red kite in Switzerland, process-explicit dSDMs can outperform correlative approaches because they do not make the equilibrium assumption. Our model also showed clear advantages over the dynamic occupancy models in Briscoe et al. (2021), likely due to the explicit consideration of spatially-explicit processes such as density-dependence in population dynamics and dispersal.

According to the future predictions of our model, the Swiss red kite population is expected to expand into the entire Swiss plateau and reach its equilibrium density within the next 30 years, then totalling a population size of around 7000 breeding pairs. With the calibrated model, the population trend under certain scenarios can be explored, for example habitat changes or modifications in single demographic rates induced by conservation measures. However, our dSDM implementation is restricted by its underlying habitat map, which was fitted with a land cover-based cSDM from recent Atlas data. It is possible that suitable but not yet occupied parts of the red kite niche were missed and therefore the future range would be underestimated by the predictions. Further, the observed increases in range and density may in part be fueled by individuals that were not recruited in the study region but immigrated from surrounding high-density populations that were not considered in the model. In the future, climate change may create new suitable areas in higher altitudes of the Alps than those that are currently occupied. This limitation can be circumvented by using a habitat model that does not rely on the equilibrium assumption, e.g. a rule-based model derived from knowledge about the species' habitat requirements or a eco-physiological SDM (Kearney & Porter, 2009). More complexity and mechanistic understanding could be incorporated by substituting the habitat model with direct relationships of species traits like demographic rates with environmental variables, thereby effectively constructing a demographic range model (Schurr et al., 2012). The inverse calibration of IBMs from observational data is also possible with other methods like pattern-oriented modelling (POM; Grimm et al., 2005; Mortensen et al., 2021) or approximate Bayesian computation (ABC; Beaumont, 2010; Hauenstein et al., 2019), the latter of which has already been demonstrated in the RangeShifter model

(Dominguez Almela et al., 2020). Independent of the chosen calibration method will the accurate parameterisation of dynamic and mechanistic SDMs remain a challenge until the paucity of high-quality ecological and monitoring data is alleviated (Oliver et al., 2012; Kissling et al., 2018). Further, the type of data collected within monitoring programs plays an important role as all model output quantities could potentially be used for inverse parameterisation. In our case study, for example, the abundances of juveniles and sub-adults were output from the IBM but could not be used for calibration because age classes are not distinguished in our surveys. Generally, the high uncertainties in parameter estimates caused by data limitations translate to large credibility intervals in model predictions, reducing the utility for conservation applications. Here, it is a clear advantage of the Bayesian framework that sources of prediction uncertainty are explicitly quantified and can thus be addressed.

In conclusion, our case study of the red kite in Switzerland shows how an individual-based dSDM can be built with RangeShiftR, calibrated using Bayesian inference, and validated by cross-validation. We derived prior parameter estimates for all process parameters from empirical data and assessed how their distributions and the resulting model predictions changed after fitting them to monitoring data. Only a subset of parameters responded substantially to the calibration, highlighting the importance of well established priors. Still, the model fit and prediction accuracy improved greatly. Which parameters of a dSDM can be successfully calibrated depends on the available calibration data. Well calibrated and validated process-based models offer compelling advantages over the currently most common static models. They are able to inform science-based management decisions and the design of proactive conservation measures (Zurell et al., 2022). Future progress in this field should be directed towards developing more flexible and accessible modelling tools, assessing their data requirements for effective parameterisation, and validating them against independent targets.

Acknowledgements

AM and DZ were supported by Deutsche Forschungsgemeinschaft (DFG) under grant agreement No. ZU 361/1-1.

Conflict of Interest statement

The authors have no conflict of interest to declare.

Author Contributions

A.-K. Malchow: Conceptualization (equal), Formal Analysis (lead), Methodology (equal), Software (lead), Data Curation (equal), Visualization (lead), Writing – Original Draft Preparation (lead), Writing – Review & Editing (equal).
G. Fandos: Conceptualization (equal, Methodology (equal), Writing – Review & Editing (equal).
U. G. Kormann: Conceptualization (equal), Data Curation (equal), Methodology (equal), Writing – Review & Editing (equal).
M. Grüebler: Conceptualization (equal), Data Curation (equal), Methodology (equal), Writing – Review & Editing (equal).
M. Kéry: Conceptualization (equal), Data Curation (equal), Writing – Review & Editing (equal).
F. Hartig: Conceptualization (equal), Formal Analysis (support), Methodology (equal), Supervision (support), Writing – Review & Editing (equal).
D. Zurell: Conceptualization (equal), Methodology (equal), Funding acquisition (lead), Supervision (lead), Writing – Review & Editing (equal).

Data Availability

`https://github.com/UP-macroecology/Malchow_IBMcalibration_2022`. Upon acceptance, we will create a permanent Zenodo archive and provide its DOI. The utilised R-packages are open-source software: RangeShiftR is available from GitHub. For this study, a tagged development version was used that is available at: `https://github.com/RangeShifter/RangeShiftR-package/releases/tag/v.1.1-beta.0`. BayesianTools is available directly from CRAN or from GitHub under `https://github.com/florianhartig/BayesianTools`.

References

Aebischer, A. and Scherler, P. (2021). *Der Rotmilan - Ein Greifvogel im Aufwind*. 1st ed. Bern: Haupt Verlag. 232 pp. ISBN: 978-3-258-08249-3.

Araújo, M. B., Pearson, R. G., Thuiller, W., and Erhard, M. (2005). "Validation of species–climate impact models under climate change". *Global Change Biology* 11.9, pp. 1504–1513. ISSN: 1365-2486. DOI: `10.1111/j.1365-2486.2005.01000.x`.

Araújo, M. B. and Peterson, A. T. (2012). "Uses and misuses of bioclimatic envelope modeling". *Ecology* 93.7, pp. 1527–1539. ISSN: 1939-9170. DOI: 10.1890/11-1930.1.

Barber-O'Malley, B., Lassalle, G., Chust, G., Diaz, E., O'Malley, A., Paradinas Blázquez, C., Pórtoles Marquina, J., and Lambert, P. (2022). "HyDiaD: A hybrid species distribution model combining dispersal, multi-habitat suitability, and population dynamics for diadromous species under climate change scenarios". *Ecological Modelling* 470, p. 109997. ISSN: 0304-3800. DOI: 10.1016/j.ecolmodel.2022.109997.

Baucks, C. (2018). "The effect of food supplementation on range use of breeding red kites (Milvus milvus) in Switzerland". Master thesis. Master thesis. Swiss Ornithological Institute Sempach.

Beaumont, M. A. (2010). "Approximate Bayesian Computation in Evolution and Ecology". *Annual Review of Ecology, Evolution, and Systematics* 41.1, pp. 379–406. ISSN: 1543-592X, 1545-2069. DOI: 10.1146/annurev-ecolsys-102209-144621.

Bellebaum, J., Korner-Nievergelt, F., Dürr, T., and Mammen, U. (2013). "Wind turbine fatalities approach a level of concern in a raptor population". *Journal for Nature Conservation* 21.6, pp. 394–400. ISSN: 1617-1381. DOI: 10.1016/j.jnc.2013.06.001.

BirdLife International (2021). *Species factsheet: Milvus milvus*. Cambridge, U.K: BirdLife International.

Bocedi, G., Palmer, S. C. F., Malchow, A.-K., Zurell, D., Watts, K., and Travis, J. M. J. (2021). "RangeShifter 2.0: an extended and enhanced platform for modelling spatial eco-evolutionary dynamics and species' responses to environmental changes". *Ecography* 44.10, pp. 1453–1462. ISSN: 1600-0587. DOI: 10.1111/ecog.05687.

Bolam, F. C. et al. (2021). "How many bird and mammal extinctions has recent conservation action prevented?" *Conservation Letters* 14.1, e12762. ISSN: 1755-263X. DOI: 10.1111/conl.12762.

Braak, C. J. F. ter and Vrugt, J. A. (2008). "Differential Evolution Markov Chain with snooker updater and fewer chains". *Statistics and Computing* 18.4, pp. 435–446. ISSN: 1573-1375. DOI: 10.1007/s11222-008-9104-9.

Briscoe, N. J., Zurell, D., Elith, J., König, C., Fandos, G., Malchow, A.-K., Kéry, M., Schmid, H., and Guillera-Arroita, G. (2021). "Can dynamic occupancy models improve predictions

of species' range dynamics? A test using Swiss birds". *Global Change Biology* 27.18, pp. 4269–4282. ISSN: 1365-2486. DOI: 10.1111/gcb.15723.

Briscoe, N. J. et al. (2019). "Forecasting species range dynamics with process-explicit models: matching methods to applications". *Ecology Letters* 22.11, pp. 1940–1956. ISSN: 1461-0248. DOI: 10.1111/ele.13348.

Broms, K. M., Hooten, M. B., Johnson, D. S., Altwegg, R., and Conquest, L. L. (2016). "Dynamic occupancy models for explicit colonization processes". *Ecology* 97.1, pp. 194–204. ISSN: 00129658. DOI: 10.1890/15-0416.1.

Cailleret, M., Bircher, N., Hartig, F., Hülsmann, L., and Bugmann, H. (2020). "Bayesian calibration of a growth-dependent tree mortality model to simulate the dynamics of European temperate forests". *Ecological Applications* 30.1, e02021. ISSN: 1939-5582. DOI: 10.1002/eap.2021.

Cereghetti, E., Scherler, P., Fattebert, J., and Grüebler, M. U. (2019). "Quantification of anthropogenic food subsidies to an avian facultative scavenger in urban and rural habitats". *Landscape and Urban Planning* 190, p. 103606. ISSN: 0169-2046. DOI: 10.1016/j.landurbplan.2019.103606.

DeAngelis, D. L. and Mooij, W. M. (2005). "Individual-Based Modeling of Ecological and Evolutionary Processes". *Annual Review of Ecology, Evolution, and Systematics* 36.1, pp. 147–168. ISSN: 1543-592X, 1545-2069. DOI: 10.1146/annurev.ecolsys.36.102003.152644.

Díaz, S. et al. (2019). "Pervasive human-driven decline of life on Earth points to the need for transformative change". *Science* 366.6471, eaax3100. DOI: 10.1126/science.aax3100.

Dominguez Almela, V., Palmer, S. C. F., Gillingham, P. K., Travis, J. M. J., and Britton, J. R. (2020). "Integrating an individual-based model with approximate Bayesian computation to predict the invasion of a freshwater fish provides insights into dispersal and range expansion dynamics". *Biological Invasions* 22.4, pp. 1461–1480. ISSN: 1573-1464. DOI: 10.1007/s10530-020-02197-6.

Dormann, C. F., Schymanski, S. J., Cabral, J., Chuine, I., Graham, C., Hartig, F., Kearney, M., Morin, X., Römermann, C., Schröder, B., and Singer, A. (2012). "Correlation and process in species distribution models: bridging a dichotomy". *Journal of Biogeography* 39.12, pp. 2119–2131. ISSN: 1365-2699. DOI: 10.1111/j.1365-2699.2011.02659.x.

Dormann, C. F. et al. (2007). "Methods to account for spatial autocorrelation in the analysis of species distributional data: a review". *Ecography* 30.5, pp. 609–628. ISSN: 1600-0587. DOI: 10.1111/j.2007.0906-7590.05171.x.

Dormann, C. F. et al. (2013). "Collinearity: a review of methods to deal with it and a simulation study evaluating their performance". *Ecography* 36.1, pp. 27–46. ISSN: 1600-0587. DOI: 10.1111/j.1600-0587.2012.07348.x.

Duarte, C. M., Agusti, S., Barbier, E., Britten, G. L., Castilla, J. C., Gattuso, J.-P., Fulweiler, R. W., Hughes, T. P., Knowlton, N., Lovelock, C. E., Lotze, H. K., Predragovic, M., Poloczanska, E., Roberts, C., and Worm, B. (2020). "Rebuilding marine life". *Nature* 580.7801, pp. 39–51. ISSN: 1476-4687. DOI: 10.1038/s41586-020-2146-7.

Elith, J. and Leathwick, J. R. (2009). "Species Distribution Models: Ecological Explanation and Prediction Across Space and Time". *Annual Review of Ecology, Evolution, and Systematics* 40.1, pp. 677–697. ISSN: 1543-592X, 1545-2069. DOI: 10.1146/annurev.ecolsys.110308.120159.

European Union (2022). *Copernicus Land Monitoring Service*.

Evans, I. M. and Pienkowski, M. (1991). "World status of the Red Kite". *British Birds* 84, pp. 171–187.

Fordham, D. A., Akçakaya, H. R., Araújo, M. B., Keith, D. A., and Brook, B. W. (2013). "Tools for integrating range change, extinction risk and climate change information into conservation management". *Ecography* 36.9, pp. 956–964. ISSN: 1600-0587. DOI: 10.1111/j.1600-0587.2013.00147.x.

Fordham, D. A., Haythorne, S., Brown, S. C., Buettel, J. C., and Brook, B. W. (2021). "poems: R package for simulating species' range dynamics using pattern-oriented validation". *Methods in Ecology and Evolution* 12.12, pp. 2364–2371. ISSN: 2041-210X. DOI: 10.1111/2041-210X.13720.

Franklin, J. (2013). "Species distribution models in conservation biogeography: developments and challenges". *Diversity and Distributions* 19.10, pp. 1217–1223. ISSN: 13669516. DOI: 10.1111/ddi.12125.

Gallien, L., Münkemüller, T., Albert, C. H., Boulangeat, I., and Thuiller, W. (2010). "Predicting potential distributions of invasive species: where to go from here?" *Diversity and Distributions* 16.3, pp. 331–342. ISSN: 1472-4642. DOI: 10.1111/j.1472-4642.2010.00652.x.

Gelman, A. and Rubin, D. B. (1992). "Inference from Iterative Simulation Using Multiple Sequences". *Statistical Science* 7.4, pp. 457–472. ISSN: 0883-4237, 2168-8745. DOI: 10.1214/ss/1177011136.

Grimm, V. et al. (2020). "The ODD protocol for describing agent-based and other simulation models: A second update to improve clarity, replication, and structural realism". *Journal of Artificial Societies and Social Simulation* 23.2. ISSN: 1460-7425.

Grimm, V., Revilla, E., Berger, U., Jeltsch, F., Mooij, W. M., Railsback, S. F., Thulke, H.-H., Weiner, J., Wiegand, T., and DeAngelis, D. L. (2005). "Pattern-Oriented Modeling of Agent-Based Complex Systems: Lessons from Ecology". *Science* 310.5750, pp. 987–991. ISSN: 0036-8075, 1095-9203. DOI: 10.1126/science.1116681.

Guisan, A. and Thuiller, W. (2005). "Predicting species distribution: offering more than simple habitat models". *Ecology Letters* 8.9, pp. 993–1009. ISSN: 1461-0248. DOI: 10.1111/j.1461-0248.2005.00792.x.

Guisan, A. et al. (2013). "Predicting species distributions for conservation decisions". *Ecology Letters* 16.12. Ed. by H. Arita, pp. 1424–1435. ISSN: 1461-023X, 1461-0248. DOI: 10.1111/ele.12189.

Hartig, F., Dyke, J., Hickler, T., Higgins, S. I., O'Hara, R. B., Scheiter, S., and Huth, A. (2012). "Connecting dynamic vegetation models to data – an inverse perspective". *Journal of Biogeography* 39.12, pp. 2240–2252. ISSN: 1365-2699. DOI: 10.1111/j.1365-2699.2012.02745.x.

Hartig, F., Minunno, F., and Paul, S. (2019). "BayesianTools: General-purpose MCMC and SMC Samplers and Tools for Bayesian Statistics". *R package version 0.1.7*.

Hauenstein, S., Fattebert, J., Grüebler, M. U., Naef-Daenzer, B., Pe'er, G., and Hartig, F. (2019). "Calibrating an individual-based movement model to predict functional connectivity for little owls". *Ecological Applications* 29.4, e01873. ISSN: 1939-5582. DOI: 10.1002/eap.1873.

Heard, G. W., McCarthy, M. A., Scroggie, M. P., Baumgartner, J. B., and Parris, K. M. (2013). "A Bayesian model of metapopulation viability, with application to an endangered amphibian". *Diversity and Distributions* 19.5, pp. 555–566. ISSN: 1472-4642. DOI: 10.1111/ddi.12052.

Hoffmann, M. et al. (2010). "The Impact of Conservation on the Status of the World's Vertebrates". *Science* 330.6010, pp. 1503–1509. DOI: 10.1126/science.1194442.

Jaatinen, K., Westerbom, M., Norkko, A., Mustonen, O., and Koons, D. N. (2021). "Detrimental impacts of climate change may be exacerbated by density-dependent population regulation in blue mussels". *Journal of Animal Ecology* 90.3, pp. 562–573. ISSN: 1365-2656. DOI: 10.1111/1365-2656.13377.

Karger, D. N., Conrad, O., Böhner, J., Kawohl, T., Kreft, H., Soria-Auza, R. W., Zimmermann, N. E., Linder, H. P., and Kessler, M. (2016). *CHELSA climatologies at high resolution for the earth's land surface areas (Version 1.1)*. DOI: 10.1594/WDCC/CHELSA_v1_1.

– (2017). "Climatologies at high resolution for the earth's land surface areas". *Scientific Data* 4.1, p. 170122. ISSN: 2052-4463. DOI: 10.1038/sdata.2017.122.

Katzenberger, J., Gottschalk, E., Balkenhol, N., and Waltert, M. (2019). "Long-term decline of juvenile survival in German Red Kites". *Journal of Ornithology* 160.2, pp. 337–349. ISSN: 2193-7206. DOI: 10.1007/s10336-018-1619-z.

Kearney, M. and Porter, W. (2009). "Mechanistic niche modelling: combining physiological and spatial data to predict species' ranges". *Ecology Letters* 12.4, pp. 334–350. ISSN: 1461-0248. DOI: 10.1111/j.1461-0248.2008.01277.x.

Keith, D. A., Akçakaya, H. R., Thuiller, W., Midgley, G. F., Pearson, R. G., Phillips, S. J., Regan, H. M., Araújo, M. B., and Rebelo, T. G. (2008). "Predicting extinction risks under climate change: coupling stochastic population models with dynamic bioclimatic habitat models". *Biology Letters* 4.5, pp. 560–563. ISSN: 1744-9561. DOI: 10.1098/rsbl.2008.0049.

Kéry, M., Guillera-Arroita, G., and Lahoz-Monfort, J. J. (2013). "Analysing and mapping species range dynamics using occupancy models". *Journal of Biogeography* 40.8, pp. 1463–1474. ISSN: 1365-2699. DOI: 10.1111/jbi.12087.

Kissling, W. D. et al. (2018). "Building essential biodiversity variables (EBVs) of species distribution and abundance at a global scale". *Biological Reviews* 93.1, pp. 600–625. ISSN: 1469-185X. DOI: 10.1111/brv.12359.

Knaus, P., Strebel, N., and Sattler, T. (2022). *The State of Birds in Switzerland 2022*. Sempach: Swiss Ornithological Institute.

Knaus, P., Jérôme, G., Sattler, T., Wechsler, S., Kéry, M., Strebel, N., and Antoniazza, S. (2018). *Schweizer Brutvogelatlas 2013-2016*. Sempach, Schweiz: Schweizerische Vogelwarte. ISBN: 978-3-85949-009-3.

Luengo, D., Martino, L., Bugallo, M., Elvira, V., and Särkkä, S. (2020). "A survey of Monte Carlo methods for parameter estimation". *EURASIP Journal on Advances in Signal Processing* 2020.1, p. 25. ISSN: 1687-6180. DOI: 10.1186/s13634-020-00675-6.

Malchow, A.-K., Bocedi, G., Palmer, S. C. F., Travis, J. M. J., and Zurell, D. (2021). "RangeShiftR: an R package for individual-based simulation of spatial eco-evolutionary dynamics and species' responses to environmental changes". *Ecography* 44.10, pp. 1443–1452. ISSN: 1600-0587. DOI: 10.1111/ecog.05689.

Marion, G., McInerny, G. J., Pagel, J., Catterall, S., Cook, A. R., Hartig, F., and O'Hara, R. B. (2012). "Parameter and uncertainty estimation for process-oriented population and distribution models: data, statistics and the niche". *Journal of Biogeography* 39.12, pp. 2225–2239. ISSN: 1365-2699. DOI: 10.1111/j.1365-2699.2012.02772.x.

Mattsson, B. J. et al. (2022). "Enhancing monitoring and transboundary collaboration for conserving migratory species under global change: The priority case of the red kite". *Journal of Environmental Management* 317, p. 115345. ISSN: 0301-4797. DOI: 10.1016/j.jenvman.2022.115345.

Morris, M. D. (1991). "Factorial Sampling Plans for Preliminary Computational Experiments". *Technometrics* 33.2, pp. 161–174. ISSN: 0040-1706. DOI: 10.1080/00401706.1991.10484804.

Mortensen, L. O., Chudzinska, M. E., Slabbekoorn, H., and Thomsen, F. (2021). "Agent-based models to investigate sound impact on marine animals: bridging the gap between effects on individual behaviour and population level consequences". *Oikos* 130.7, pp. 1074–1086. ISSN: 1600-0706. DOI: 10.1111/oik.08078.

Nachtigall, W. (2008). "Der Rotmilan (Milvus milvus, L. 1758) in Sachsen und Südbrandenburg–Untersuchungen zu Verbreitung und Ökologie". *Diss., Univ. Halle-Wittenberg*.

Nägeli, M., Scherler, P., Witczak, S., Catitti, B., Aebischer, A., Bergen, V. van, Kormann, U., and Grüebler, M. U. (2021). "Weather and food availability additively affect reproductive output in an expanding raptor population". *Oecologia*. ISSN: 1432-1939. DOI: 10.1007/s00442-021-05076-6.

Newbold, T. et al. (2015). "Global effects of land use on local terrestrial biodiversity". *Nature* 520.7545, pp. 45–50. ISSN: 1476-4687. DOI: 10.1038/nature14324.

Newson, R. (2006). "Confidence Intervals for Rank Statistics: Somers' D and Extensions". *The Stata Journal* 6.3, pp. 309–334. ISSN: 1536-867X. DOI: 10.1177/1536867X0600600302.

Newton, I., Davis, P., and Davis, J. (1989). "Age of first breeding, dispersal and survival of Red Kites Milvus milvus in Wales". *Ibis* 131.1, pp. 16–21.

Oliver, T. H., Gillings, S., Girardello, M., Rapacciuolo, G., Brereton, T. M., Siriwardena, G. M., Roy, D. B., Pywell, R., and Fuller, R. J. (2012). "Population density but not stability can be predicted from species distribution models". *Journal of Applied Ecology* 49.3, pp. 581–590. ISSN: 1365-2664. DOI: 10.1111/j.1365-2664.2012.02138.x.

Pellissier, L., Rohr, R. P., Ndiribe, C., Pradervand, J.-N., Salamin, N., Guisan, A., and Wisz, M. (2013). "Combining food web and species distribution models for improved community projections". *Ecology and Evolution* 3.13, pp. 4572–4583. ISSN: 2045-7758. DOI: 10.1002/ece3.843.

R Core Team (2020). *R: A Language and Environment for Statistical Computing*. Vienna, Austria: R Foundation for Statistical Computing.

Railsback, S. F. and Grimm, V. (2019). *Agent-Based and Individual-Based Modeling: A Practical Introduction, Second Edition*. Princeton University Press. 359 pp. ISBN: 978-0-691-19004-4.

Risk, B. B., Valpine, P. de, and Beissinger, S. R. (2011). "A robust-design formulation of the incidence function model of metapopulation dynamics applied to two species of rails". *Ecology* 92.2, pp. 462–474. ISSN: 1939-9170. DOI: 10.1890/09-2402.1.

Roberts, D. R., Bahn, V., Ciuti, S., Boyce, M. S., Elith, J., Guillera-Arroita, G., Hauenstein, S., Lahoz-Monfort, J. J., Schröder, B., Thuiller, W., Warton, D. I., Wintle, B. A., Hartig, F., and Dormann, C. F. (2017). "Cross-validation strategies for data with temporal, spatial, hierarchical, or phylogenetic structure". *Ecography* 40.8, pp. 913–929. ISSN: 1600-0587. DOI: 10.1111/ecog.02881.

Rodríguez, L., García, J. J., Carreño, F., and Martínez, B. (2019). "Integration of physiological knowledge into hybrid species distribution modelling to improve forecast of distributional shifts of tropical corals". *Diversity and Distributions* 25.5, pp. 715–728. ISSN: 1472-4642. DOI: 10.1111/ddi.12883.

Santos, E. P., Wagner, H. H., Ferraz, S. F. B., and Siqueira, T. (2020). "Interactive persistent effects of past land-cover and its trajectory on tropical freshwater biodiversity". *Journal of Applied Ecology* 57.11, pp. 2149–2158. ISSN: 1365-2664. DOI: 10.1111/1365-2664.13717.

Schaub, M. (2012). "Spatial distribution of wind turbines is crucial for the survival of red kite populations". *Biological Conservation* 155, pp. 111–118. ISSN: 0006-3207. DOI: 10.1016/j.biocon.2012.06.021.

Schmid, H., Luder, R., Naef-Daenzer, B., Graf, R., and Zbinden, N. (1998). *Schweizer Brutvogelatlas 1993–1996*. Sempach, Schweiz: Schweizerische Vogelwarte. ISBN: 978-3-9521064-5-7.

Schmid, H., Zbinden, N., and Keller, V. (2004). *Überwachung der Bestandsentwicklung häufiger Brutvögel in der Schweiz*. Sempach: Schweizerische Vogelwarte.

Schurr, F. M., Pagel, J., Cabral, J. S., Groeneveld, J., Bykova, O., O'Hara, R. B., Hartig, F., Kissling, W. D., Linder, H. P., Midgley, G. F., Schröder, B., Singer, A., and Zimmermann, N. E. (2012). "How to understand species' niches and range dynamics: a demographic research agenda for biogeography". *Journal of Biogeography* 39.12, pp. 2146–2162. ISSN: 1365-2699. DOI: 10.1111/j.1365-2699.2012.02737.x.

Schweiger, O., Heikkinen, R. K., Harpke, A., Hickler, T., Klotz, S., Kudrna, O., Kühn, I., Pöyry, J., and Settele, J. (2012). "Increasing range mismatching of interacting species under global change is related to their ecological characteristics". *Global Ecology and Biogeography* 21.1, pp. 88–99. ISSN: 1466-8238. DOI: 10.1111/j.1466-8238.2010.00607.x.

Selwood, K. E., McGeoch, M. A., and Mac Nally, R. (2015). "The effects of climate change and land-use change on demographic rates and population viability". *Biological Reviews* 90.3, pp. 837–853. ISSN: 1469-185X. DOI: 10.1111/brv.12136.

Semper-Pascual, A., Burton, C., Baumann, M., Decarre, J., Gavier-Pizarro, G., Gómez-Valencia, B., Macchi, L., Mastrangelo, M. E., Pötzschner, F., Zelaya, P. V., and Kuemmerle, T. (2021). "How do habitat amount and habitat fragmentation drive time-delayed responses of biodiversity to land-use change?" *Proceedings of the Royal Society B: Biological Sciences* 288.1942, p. 20202466. DOI: 10.1098/rspb.2020.2466.

Sergio, F., Tavecchia, G., Blas, J., Tanferna, A., and Hiraldo, F. (2021). "Demographic modeling to fine-tune conservation targets: importance of pre-adults for the decline of an

endangered raptor". *Ecological Applications* 31.3, e2266. ISSN: 1939-5582. DOI: https://doi.org/10.1002/eap.2266.

Singer, A., Schweiger, O., Kühn, I., and Johst, K. (2018). "Constructing a hybrid species distribution model from standard large-scale distribution data". *Ecological Modelling* 373, pp. 39–52. ISSN: 0304-3800. DOI: 10.1016/j.ecolmodel.2018.02.002.

Smolik, M., Dullinger, S., Essl, F., Kleinbauer, I., Leitner, M., Peterseil, J., Stadler, L.-M., and Vogl, G. (2010). "Integrating species distribution models and interacting particle systems to predict the spread of an invasive alien plant". *Journal of Biogeography* 37.3, pp. 411–422. ISSN: 1365-2699. DOI: 10.1111/j.1365-2699.2009.02227.x.

Thompson, B. K., Olden, J. D., and Converse, S. J. (2021). "Mechanistic invasive species management models and their application in conservation". *Conservation Science and Practice* 3.11, e533. ISSN: 2578-4854. DOI: 10.1111/csp2.533.

Travis, J. M. J., Mustin, K., Bartoń, K. A., Benton, T. G., Clobert, J., Delgado, M. M., Dytham, C., Hovestadt, T., Palmer, S. C. F., Dyck, H. V., and Bonte, D. (2012). "Modelling dispersal: an eco-evolutionary framework incorporating emigration, movement, settlement behaviour and the multiple costs involved". *Methods in Ecology and Evolution* 3.4, pp. 628–641. ISSN: 2041-210X. DOI: 10.1111/j.2041-210X.2012.00193.x.

Urban, M. C. et al. (2016). "Improving the forecast for biodiversity under climate change". *Science* 353.6304. ISSN: 0036-8075, 1095-9203. DOI: 10.1126/science.aad8466.

Vehtari, A., Gelman, A., and Gabry, J. (2017). "Practical Bayesian model evaluation using leave-one-out cross-validation and WAIC". *Statistics and Computing* 27.5, pp. 1413–1432. ISSN: 1573-1375. DOI: 10.1007/s11222-016-9696-4.

Vehtari, A., Gelman, A., Simpson, D., Carpenter, B., and Bürkner, P.-C. (2021). "Rank-Normalization, Folding, and Localization: An Improved R^ for Assessing Convergence of MCMC (with Discussion)". *Bayesian Analysis* 16.2, pp. 667–718. ISSN: 1936-0975, 1931-6690. DOI: 10.1214/20-BA1221.

Visintin, C., Briscoe, N. J., Woolley, S. N. C., Lentini, P. E., Tingley, R., Wintle, B. A., and Golding, N. (2020). "steps: Software for spatially and temporally explicit population simulations". *Methods in Ecology and Evolution* 11.4, pp. 596–603. ISSN: 2041-210X. DOI: 10.1111/2041-210X.13354.

Warne, D. J., Baker, R. E., and Simpson, M. J. (2020). "A practical guide to pseudo-marginal methods for computational inference in systems biology". *Journal of Theoretical Biology* 496, p. 110255. ISSN: 0022-5193. DOI: 10.1016/j.jtbi.2020.110255.

Watts, K., Whytock, R. C., Park, K. J., Fuentes-Montemayor, E., Macgregor, N. A., Duffield, S., and McGowan, P. J. K. (2020). "Ecological time lags and the journey towards conservation success". *Nature Ecology & Evolution* 4.3, pp. 304–311. ISSN: 2397-334X. DOI: 10.1038/s41559-019-1087-8.

Wenger, S. J. and Olden, J. D. (2012). "Assessing transferability of ecological models: an underappreciated aspect of statistical validation". *Methods in Ecology and Evolution* 3.2, pp. 260–267. ISSN: 2041-210X. DOI: 10.1111/j.2041-210X.2011.00170.x.

Zurell, D., König, C., Malchow, A.-K., Kapitza, S., Bocedi, G., Travis, J., and Fandos, G. (2022). "Spatially explicit models for decision-making in animal conservation and restoration". *Ecography* 2022.4. ISSN: 1600-0587. DOI: 10.1111/ecog.05787.

Zylstra, E. R. and Zipkin, E. F. (2021). "Accounting for sources of uncertainty when forecasting population responses to climate change". *Journal of Animal Ecology* 90.3, pp. 558–561. ISSN: 1365-2656. DOI: 10.1111/1365-2656.13443.